ORIGINAL ARTICLE

UDC: 616.314-089.843-092.9
DOI: 10.2298/VSP121003034D

Implant stability and marginal bone level of microgrooved zirconia dental implants: A 3-month experimental study on dogs

Implantatna stabilnost i nivo marginalne kosti kod cirkonijum endoosealnih implantata sa mikrostrukturiranom površinom: tromesečna eksperimentalna studija na psima

Rafael Arcesio Delgado-Ruíz*, Aleksa Marković†, José Luís Calvo-Guirado*, Zoran Lazić‡, Adriano Piattelli§, Daniele Boticelli¤, José Eduardo Maté-Sánchez*, Bruno Negri*, María Piedad Ramírez-Fernández*, Tijana Mišić†

***Faculty of Medicine and Dentistry, University of Murcia, Murcia, Spain; †Faculty of Dentistry, University of Belgrade, Belgrade, Serbia; ‡Clinic of Maxillofacial, Oral Surgery and Implantology, Military Medical Academy, Belgrade, Serbia; ¤Faculty of Odontology, Göeteborg University, Göeteborg, Sweden; §Dental School, University of Chieti-Pescara, Chieti, Italy**

Abstract

Background/Aim. The modification of implant surfaces could affect mechanical implant stability as well as dynamics and quality of peri-implant bone healing. The aim of this 3-month experimental study in dogs was to investigate implant stability, marginal bone levels and bone tissue response to zirconia dental implants with two laser-micro-grooved intraosseous surfaces in comparison with nongrooved sandblasted zirconia and sandblasted, high-temperature etched titanium implants. **Methods.** Implant surface characterization was performed using optical interferometric profilometry and energy dispersive X-ray spectroscopy. A total of 96 implants (4 mm in diameter and 10 mm in length) were inserted randomly in both sides of the lower jaw of 12 Fox Hound dogs divided into groups of 24 each: the control (titanium), the group A (sandblasted zirconia), the group B (sandblasted zirconia plus microgrooved neck) and the group C (sandblasted zirconia plus all microgrooved). All the implants were immediately loaded. Insertion torque, periotest values, radiographic crestal bone level and removal torque were recorded during the 3-month follow-up. Qualitative scanning electon microscope (SEM) analysis of the bone-implant interfaces of each group was performed. **Results.** Insertion torque values were higher in the group C and control implants ($p < 0.05$). Periotest values increased in all the periods in proportion to the extent of microgrooving as follows: the group C > the control > the group B > the group A ($p < 0.05$). Radiographic measurements showed minimal crestal bone loss at 3 months for microgrooved zirconia implants (groups C and B) and control implants compared with the group A implants ($p < 0.05$). The removal torque values increased with time for all the groups as follows: the group C > the control > the group B > the group A ($p < 0.05$). SEM showed that implant surfaces of the groups B and C had an extra bone growth inside the microgrooves that corresponded to the shape and direction of the microgrooves. **Conclusion.** The addition of microgrooves to the entire intraosseous surface of zirconia dental implants enhances primary and secondary implant stability, promotes bone tissue ingrowth and preserves crestal bone levels.

Key words:
dental implants; surface properties; biomechanics; microscopy, electron, scanning; alveolar bone loss; zirconium; titanium; dogs.

Apstrakt

Uvod/Cilj. Modifikacija površine implantata može uticati na njegovu mehaničku stabilnost kao i na dinamiku i kvalitet periimplantatnog koštanog zarastanja. Cilj ove tromesečne eksperimentalne studije na psima bio je da se ispita stabilnost implantata, nivo marginalne kosti i odgovor koštanog tkiva na cirkonijum endoosealne implantate sa dve intraosealne površine mikrostrukturirane laserom u poređenju sa peskiranim cirkonijum implantatima čija površina nije mikrostrukturirana kao i sa titanijum implantatima čije su površine peskirane i nagrižene visokom temperaturom. **Metode.** Karakterizacija površine implantata učinjena je optičkom interferometrijskom profilometrijom i analizom energetskog spektra pri difrakciji X-zračenja. Ukupno 96 implantata (prečnika 4 mm i dužine 10 mm) ugrađeno je nasumično i obostrano u donju vilicu

Correspondence to: Aleksa Marković, Faculty of Dentistry, University of Belgrade, Dr Subotića 4, 11 000 Belgrade, Serbia.
Phone: +381 11 268 52 68. E-mail: maleksa64@gmail.com

kod 12 pasa (lisičara) i podeljeno u četiri grupe po 24: kontrolna (titanijum implantati); grupa A (peskirani cirkonijum implantati); grupa B (peskirani cirkonijum implantati sa mikrokanalima u koronarnoj trećini); grupa C (peskirani cirkonijum implantati sa mikrokanalima duž cele površine). Svi implantati su odmah opterećeni. Meren je obrtni momenat pri ugradnji implantata, vrednosti periotesta, radiografski nivo marginalne kosti i obrtni moment za uklanjanje implantata tokom tromesečnog perioda praćenja. Međuspoj kosti i implantata iz svake grupe ispitivan je kvalitativnom skenirajućom elektronskom mikroskopijom (SEM). **Rezultati.** Veći obrtni momenat zabeležen je pri ugradnji implantata kod grupe C i kontrolne grupe ($p < 0,05$). U ispitivanom vremenskom periodu, vrednosti periotesta uvećavale su se srazmerno obimu mikrostrukturiranja površine i to: grupa C > kontrolna grupa > grupa B > grupa A ($p < 0,05$). Radiografskom analizom utvrđen je minimalni gubitak marginalne kosti u trećem mesecu praćenja oko cirkonijum implantata sa mikrokanalima (grupa B i C) i kontrola u poređenju sa implantatima grupe A ($p < 0,05$). Vrednosti obrtnog momenta za uklanjanje implantata vremenom su se uvećavale u svim grupama na sledeći način: grupa C > kontrolna grupa > grupa B > grupa A ($p < 0,05$). Kod implantatnih površina grupa B i C, SEM je pokazala dodatni rast koštanog tkiva unutar mikrokanala koji odgovara njihovom obliku i pravcu. **Zaključak.** Formiranje mikrokanala duž cele intraosealne površine cirkonijum endoosealnih implantata povećava primarnu i sekundarnu implantatnu stabilnost, podstiče urastanje koštanog tkiva i održava nivo marginalne kosti.

Ključne reči:
implantati, stomatološki; površina, svojstva; biomehanika; mikroskopija, elektronska, skenirajuća; kost, resorpcija; cirkonijum; titanijum; psi.

Introduction

Although titanium can still be considered the reference standard material for dental implants, recent advances in the development of high mechanical strength ceramics have made them a viable alternative [1]. Yttrium partially stabilized tetragonal zirconia (Y-TZP) offers several advantages due to its flexural strength and high resistance to fracture [2, 3], favorable esthetics as well as excellent osseointegration observed in animal studies [4, 5].

Regardless of the type of implant material, rough surface achieves a great contact area with adjacent bone tissue, providing better mechanical stability of the implant which is the basic prerequisite for successful osseointegration. The implant surface modification promotes contact osteogenesis which results in accelerated and enhanced healing [6]. The topography of the coronal aspect of the implant could affect maintenance of marginal bone level [7].

However, roughening the surface of the zirconia implant is a challenge mainly due to its resistance to chemical or physical modifications. Several approaches have been proposed: chemical and pharmacological surface modification [8], sand-blasting and acid etching [9], the use of nanotechnology [10], or biomimetic coatings [11], and addition of micro and macro-retentions [12]. As a result, various degrees of surface roughness and traces of contaminants compromising implants` biocompatibility have been observed. Recently, technique for microstructuring cylindrical zirconia implants by femtosecond laser ablation has been introduced. Initial findings have shown increased surface roughness, a decrease in the presence of contaminants such as aluminum and carbon, an increase in oxygen presence and a decrease in monoclinic phase zirconia on the processed surfaces [13].

Previous studies have shown that the application of microgrooves to the implant surface can direct cellular morphology and cell migration [14, 15], improve cell adhesion [14, 16, 17] and also improve cell differentiation and mineralized matrix deposition [17, 18]. On titanium dental implant surfaces, the incorporation of microthreads [19] and microgrooves of different sizes in the neck area can guide specific cellular lines including osteoblasts (12 μm microgrooves) and fibroblasts (8 μm microgrooves), resulting in better quality connective tissue insertion and reduced crestal bone loss [20–22]. To date no research has been carried on stability variations and alterations to crestal bone for zirconia implants with the intraosseous portion microgrooved in different areas.

The aim of this 3-month experimental study in dogs was to examine zirconia dental implants with two laser-micro-grooved surfaces in terms of their stability, changes in marginal bone level and bone tissue response in comparison with nongrooved sandblasted zirconia and sandblasted, high-temperature etched titanium implants.

Methods

Twelve Fox Hound dogs of approximately one year of age, each weighting between 14 to 15 kg were used in the experiment. The Ethics Committee for Animal Research at the University of Murcia, Spain, approved the study (Murcia-November-2010 and August-2011), which followed a guidelines established by the European Union Council Directive of November 24th, 1986 (86/609/EEC).

Implants and surface characterization

A total of 104 commercially manufactured implants of 4 mm diameter and 10 mm length were used for the study. Four groups were studied: the control group – 26 titanium BlueSKY® implants (Bredent medical® GMBH & Co. KG, Senden, Germany); the group A – 26 sandblasted WhiteSKY® zirconia implants (Bredent medical® GMBH & Co. KG, Senden, Germany); the group B – 26 WhiteSKY® sandblasted zirconia implants (Bredent medical® GMBH & Co. KG, Senden, Germany) treated with femtosecond laser pulses to create 30 μm wide, 70 μm pitch length microgrooves over 2 mm of the neck area; the group C – 26 WhiteSKY® sandblasted zirconia implants (Bredent medical® GMBH & Co. KG, Senden, Germany) treated with femtosecond laser pulses to create 30 μm wide, 70 μm pitch length microgrooves over the entire intraosseous surface (Figures 1–3).

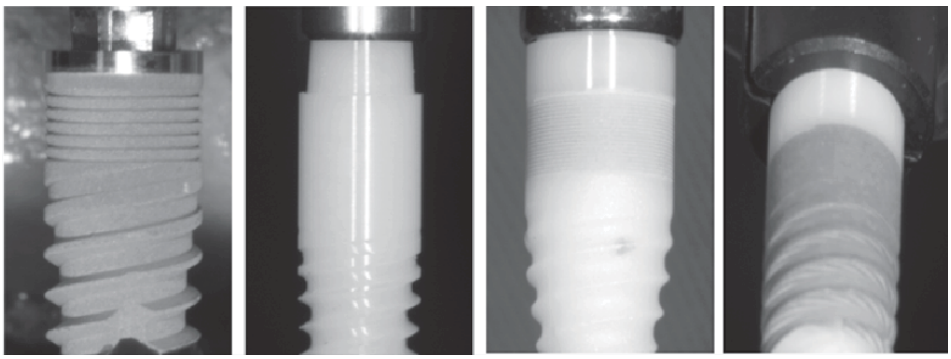

Fig. 1 – Clinical view of groups of implants used in this study. From left to right, the control (titanium implant), the group A (zirconia implant with sandblasted surface), the group B (zirconia implant with microgrooved neck), and the group C (zirconia implant all microgrooved). The zirconia laser treated implants showed a characteristic darkness area corresponding to laser microgrooved surfaces.

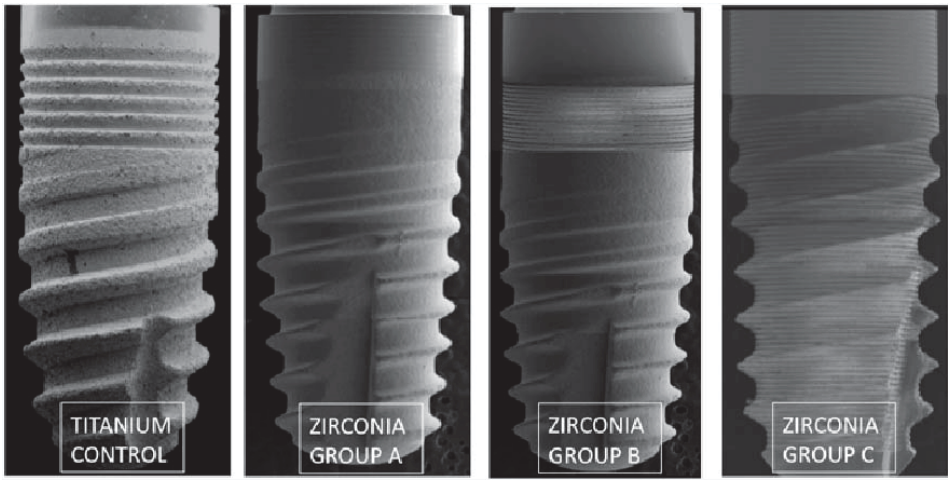

Fig. 2 – Scanning electron microscope (SEM) image composition of implants used in this study. The control implants have microthreads at neck level. All the implants have the same geometry. The laser processed surfaces of the group B and the group C showed the microgrooves at the neck level or in all surface, respectively.

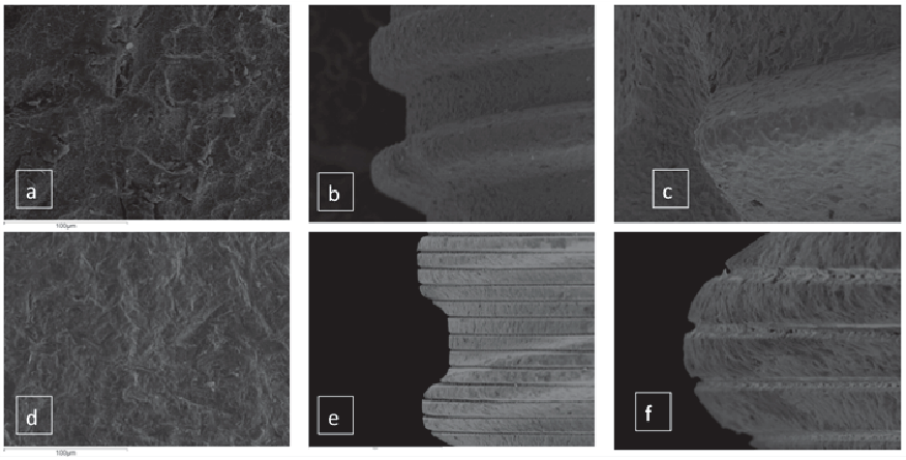

Fig. 3 – Scanning electron microscope (SEM) higher magnification reveals: a) typical image of titanium implant of the control group; b) view of threads zone in the control; c) close view of thread with typical roughness in the control; d) the group A surface with lower roughness; e) threads with microgrooves in symmetric and parallel position; f) close view of a thread with microgrooves and increased roughness inside the microgrooves and between them.

Two implants per group were used to analyze surface roughness and chemical composition of the surfaces. A Veeko NT 1100® non-contact interferometric microscope (Wyco Systems, New York, USA) was used to quantify following surface roughness parameters: Ra (average surface roughness), root mean square roughness (Rq), average maximum height of the surface (Rz), maximum height of the surface (Rt). Ten random measurements with 20.7 X magni-

fication in VSI mode were performed within the intraosseous portion of the implant surfaces. The sampling areas were 227.2 μm × 298.7 μm. Elemental chemical composition analysis was carried out by Energy Dispersive X-ray spectroscopy (EDX) using an OXFORD INCA 300 system (Oxford Instruments, UK). All specimens were coated with a thin layer of conductive carbon in a sputter-coating unit (SCD 004 Sputter-Coater with OCD 30 attachment, Bal-Tec, Vaduz, Liechtenstein). Chemical composition analysis was performed in ten sampling areas on the surfaces of the intraosseous portions.

Surgical procedure

The animals were pre-anesthetized with acepromazine (0.2–1.5% mg/kg) 10 min. before administering butorphanol (0.2 mg/kg) and medetomidine (7 mg/kg). The mixture was injected intramuscularly in the femoral quadriceps. An intravenous catheter was inserted in the cephalic vein and propophol was infused at a slow, constant rate of 0.4 mg/kg/min. Local infiltrative anesthesia was administered at the surgical sites. An intrasulcular incision was performed from distal aspect of the first mandibular premolar (P_1) to a point mesial of the second mandibular molar (M_2), bilaterally and a full thickness flaps were raised. Following tooth section the second mandibular premolars (P_2), the third mandibular premolars (P_3), the fourth mandibular premolars (P_4) and the first mandibular molars (M_1) were extracted bilaterally, using a periotome and forceps, without damaging the bony walls. Wound closure was carried out using single resorbable sutures.

During the first week after the surgery, the animals received antibiotics and analgesics: amoxicillin (500 mg, twice daily) and ibuprofen (600 mg, three times a day) *via* the systemic route. After 14 days of soft diet, a normal pellet diet was established.

After a 2-month healing period, a total of 96 implants were placed. Implant positions and implant type were determined using a random allocation software, so that each hemimandible received four implants from any group inserted randomly at P_2, P_3, P_4 and M_1 positions.

After crestal incision, a full thickness flap from distal aspect of P1 to mesial aspect of M2 medially was reflected and implant sites of 4 mm diameter and 10 mm length were prepared with strict adherence to manufacturer`s protocol (Figures 4 a-d). Each mandible received 8 cylindrical screw implants, all with the same dimensions at the intraosseous portion. Implants from the groups A, B and C were inserted with shoulders 2 mm above the osseous crest while in the control group implant shoulders were at the crestal level.

On the day of implant placement, provisional splints were made and all implants were immediately loaded (Figures 4 e-i).

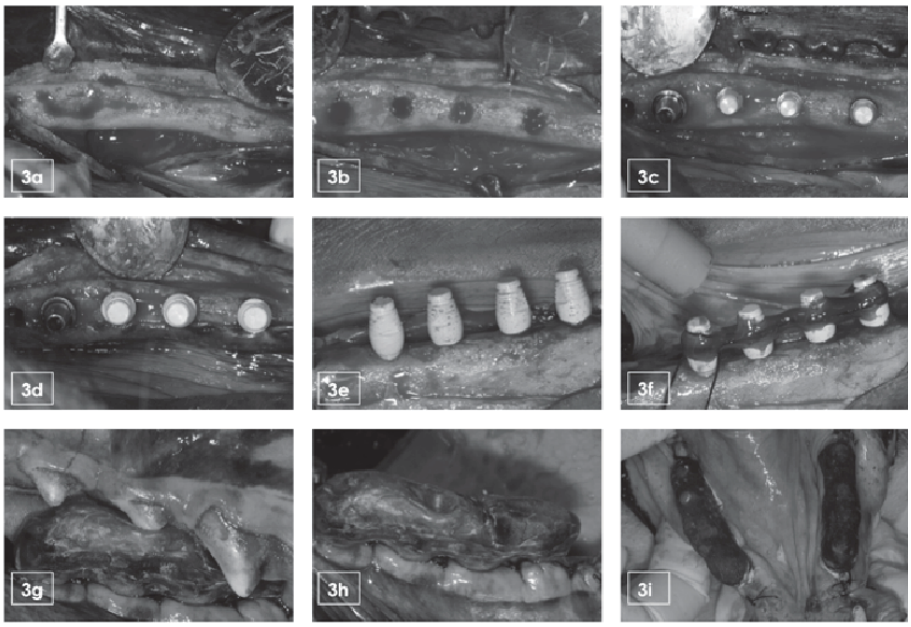

Fig. 4 – Surgical and prosthetic step-by-step procedures: a) complete open mucoperiosteal flap; b) prepared implant beds, c) randomly inserted implants: titanium implant with prosthetic abutment and zirconia implants; d) occlusal view; e) special plastic cover placed over the implants; f) implants splinted by orthodontic wires and acrylic resin; g) occlusion test; h) occlusal adjustment and gingival finishing; i) provisionalization completed, occlusal view of bilateral temporary acrylic splint.

Four animals were sacrificed for each evaluation time after the first, second and third months. The animals were pre-anesthetized following the protocol described earlier, followed by a perfusion of sodium pentothal (Abbot Laboratories, Chicago, IL, USA) through the carotid artery.

Insertion torque

Insertion torque (IT) values were measured at day 0 on 96 implants by means of an electronic instrument (FRIOS® Unit E, W&H Dental Werk GmbH, Buermoos, Austria) during low-speed insertion, registering the maximum peak (Ncm) reached at the crestal implant level.

Periotest values

The Periotest values (PTV) were registered following the animals' sacrifice at 1st, 2nd and 3rd postoperative months. For that purpose, acrylic splints that link the implant posts were removed and each extracted mandible was stabilized in a metallic support to ensure immobility. Since the zirconia implants used in this study were one-piece implants, the titanium implants of the control group received a straight titanium abutment SKY-EM00® (Bredent medical® GMBH & Co. KG, Senden, Germany) tightened to the implant with a torque of 25 Ncm in order to provide uniform conditions in terms of immediate loading and PTV testing for all experimental groups.

When the titanium abutments had been attached, the secondary stability of all implants was evaluated with a Periotest® device (Siemens, Bensheim, Germany), calibrated from -7 (maximum stability) to +7 (minimum stability) for each zirconia or titanium implant. The point of the instrument was placed perpendicularly to the middle third of the abutments' vestibular face and three evaluations were registered by a single operator, who recorded the mean value.

Radiographic crestal bone level

Radiographic crestal bone level (RCBL) interpretation was performed from digital retroalveolar radiographs at one month, 2-month and 3-month observation (Kodak Ultra-speed size II double film, Eastman Kodak, Rochester, NY). The radiographs were taken using a customized acrylic support in order to ensure reproducibility. Standardized exposure parameters and processing procedures were used. Each radiograph was then digitalized, magnified at 7 × and analyzed for changes to crestal bone levels using Image J® software (National Institutes of Health, Bethesda, Maryland, USA).

The obtained images were processed using edge-location techniques followed by color inversion and lastly a thresholding procedure was performed. Implant shoulders and the first point of crestal bone contact were localized on both the mesial and distal aspects of each implant. For zirconia implants, two points were located, one distal and one mesial, situated 2 mm from the abutment platform, coinciding with the bone crest; for titanium implants, two points were located at the implant platform, one distal, one mesial, located 1mm from the machined neck (Figures 5).

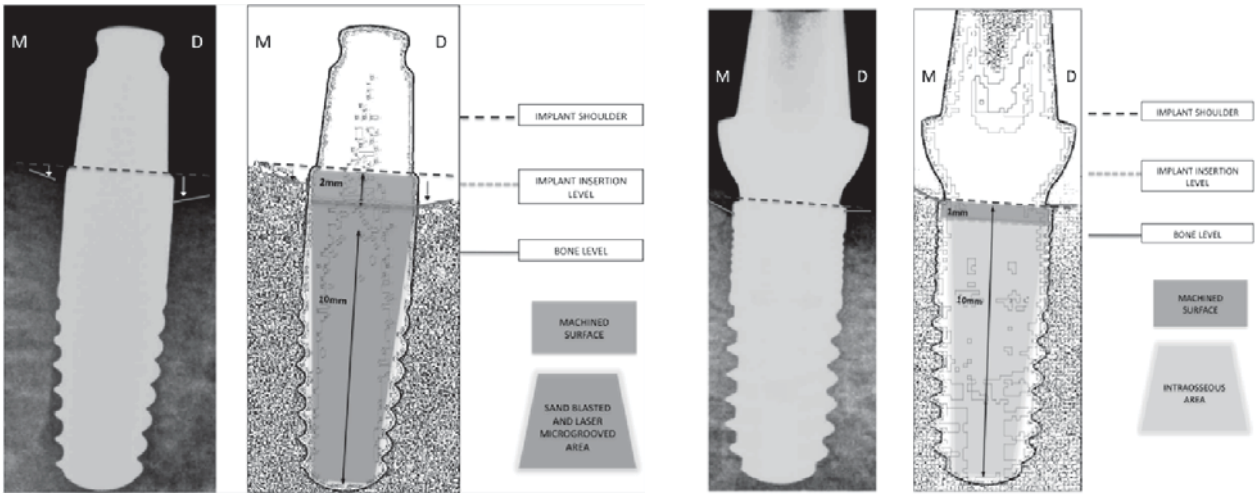

Fig. 5 – Radiographic reference points after image processing to increase detail: left) zirconia implant with landmarks; right) titanium implant with landmarks.

Removal torque

Removal torque (RT) evaluation was performed at the 1st, 2nd and 3rd postoperative months. After the meticulous elimination of all soft tissues, the mandible was fixed in a special support adding acrylic resin until the bone was covered to 1 mm below the bone crest. A Sky-WTK6 driver was used for evaluationng of titanium implants and a SKYC-WM6 driver for zirconia implants. Radiographic testing (RT) was performe by a counterclockwise rotation at a rate of 0.1°/sec using a reverse torque testing machine (Instron, Bucks, UK), recording the peak when implant movement occurred. RT was defined as the maximum torque necessary to start rotational movement of the implants. Eventual implant fracture was recorded as well.

Qualitative SEM analysis

To obtain additional information about the characteristics of the broken interfaces, qualitative SEM analysis was performed in one sample of each group after reverse torque test. A block containing the implant and surrounding bone was extracted, fixed by immersion in a 4% formalin solution, dehydrated in a graded ethanol series and embedded in light-curing resin (Technovit® 7210; Kulzer & Co, Hanau, Germany). Then, the blocks were sectioned sagittally in two halves. One was polished using a manual grinder with 800 grit silicon carbide paper, mounted on an aluminum stub and carbon coated (Polaron sputter coater, East Grinstead, Sussex UK). Samples were examined using backscattering and EDX at a working distance of 19 mm and an acceleration voltage of 20 kV under 15X, 80 X, 100 X magnification. The second was used to observe the separated implant and bone surfaces at same parameters.

Data obtained from 96 implants were analyzed using descriptive and inferential statistics. The difference in mean values of single outcome variable (IT, PTV, RCBL and RTV) between the study groups at a given time of observation was analyzed using one way ANOVA followed by Tukey`s multiple comparison test or Kruskal-Wallis test followed by Dunn's post test, depending on the nature of data distribution. Pearson correlation coefficients were calculated in order to reveal the strength of the relationship between PTV and RT, as well as RCBL and RT. *P*-values < 0.05 were considered to indicate statistically significant differences.

Results

All the animals were available for evaluation. The healing period was uneventful. The placed implants were primarily stable and subsequently osseointegrated. No implant fracture nor implant loss were detected during the study.

Surface characterization

The implants from the group C exhibited the highest values of roughness parameters (Table 1) and reduced presence of contaminants (Table 2).

Insertion torque

None of the zirconia implants has been fractured as a result of the insertion torque applied. The insertion torque values of the implants from the group C were significantly higher ascompared with each of the remaining groups ($p < 0.05$). In the group A and the group B significantly lower insertion torque values were recorded in relation to the control group ($p < 0.05$). Furthermore, the difference in mean insertion torque values between the group A and the group B was also statistically significant ($p < 0.05$) (Table 3).

Periotest results

At the first month of observation, the implants from the group C demonstrated the highest stability (ie. the lowest PT value). Dunn's multiple comparison showed a significant difference in the mean PTV between the group C and the group B ($p < 0.01$). The lowest stability was recorded in the group A and compared with the group C as well as with the controls the difference was statistically significant ($p < 0.01$), (Table 4). During a 3-month observation period, the stability of the implants in all the study groups was increasing whereas the pattern of statistical sig-

Table 1

Topographic characteristics of implants used in the study

Roughness parameters	Experimental groups			Control
	group A	group B	group C	
R_a(μm)	1.28 ± 0.2	2.43 ± 0.6*	9.50 ± 0.25*	1.78 ± 0.6
R_q(μm)	1.82 ± 0.51	3.48 ± 0.30*	11.51 ± 0.31*	2.02 ± 0.43
R_z(μm)	11.4 ± 0.6	40.42 ± 0.25*	40.74 ± 0.28*	15.8 ± 0.5
R_t(μm)	18.46 ± 0.82	52.68 ± 0.9*	60.36 ± 0.22*	23.63 ± 0.32

The results expressed as $\bar{x}$ ± SD; *$p < 0.05$.
R_a – avarage surface roughness; R_q – root mean square roughness; R_z – avarage maximum height of the surface; R_t – maximum width of the surface.

Table 2

Elements present in surface chemical composition

EDX surface analysis	Experimental groups			Control
	group A	group B	group C	
C	19.7 ± 0.8	1.6 ± 0.35*	0.3 ± 0.12*	2.3 ± 1.7
Al	4.3 ± 0.9	1.16 ± 0.2*	0.18 ± 0.1*	1.7 ± 0.3
O	12.6 ± 0.5	22.7 ± 0.2*	23.1 ± 0.12*	15 ± 0,6
Zr	60.2 ± 0.7	73.7 ± 0.15*	76.3 ± 0.2*	0
Ti	0	0	0	81 ± 1.3

The results expressed in percentages as $\bar{x}$ ± SD; *$p < 0.05$.
Other elements traces sometimes present in zirconia samples like Hf, were not detected by this probe. EDX – energy dispersive X-ray spectroscopy.

Table 3

Descriptive statistics of Insertion Torque (IT) values recorded at implant placement

Experimental group	IT(Ncm)			
	$\bar{x}$	SD	SE	Median
Control	57.10	1.80	0.51	55.76
Group A	46.08	0.70	0.20	44.87
Group B	53.20	1.30	0.37	50.98
Group C	69.60	1.20	0.34	67.82

$\bar{x}$ – mean; SD – standard deviation; SE – standard error.

Table 4

Results from the removal torque test (RT) performed at three evaluation time points

Experimental groups	RT (Ncm)		
	month 1	month 2	month 3
Group A	64.08 ± 0.42 (64.07)	78.24 ± 0.35(78.38)	199.19 ± 0.99 (199.47)
Group B	69.19 ± 0.37 (69.17)	88.82 ± 0.41 (88.86)	215.13 ± 0.99 (215.06)
Group C	84.95 ± 0.25 (85.03)	126.96 ± 0.81 (126.65)	240.15 ± 1.04 (239.90)
Control	71.25 ± 0.43 (71.28)	99.85 ± 0.44 (99.98)	226.98 ± 1.06 (226.72)

Values are expressed as $\bar{x}$ ± SD (median).

nificance of differences among the groups was the same as at the first month (Table 5).

Pearson correlation coefficient revealed a strong, highly significant and negative relation between PTV and RT (r = - 0.726; p = 0.000), whereas RCBL and RT had a moderate and positive correlation (r = 0.506; p = 0.000).

Table 5

Changes in Periotests values (PTV) during three-month follow-up

Experimental groups	PTV		
	month 1	month 2	month 3
Group A	-1.52 ± 0.01 (-1.52)	-2.17 ± 0.01 (-2.17)	-2.41 ± 0.02 (-2.41)
Group B	-1.85 ± 0.02 (-1.85)	-2.42 ± 0.01 (-2.42)	-3.11 ± 0.01 (-3.11)
Group C	-2.49 ± 0.02 (-2.5)	-4.16 ± 0.01 (-4.16)	-5.69 ± 0.03 (-5.7)
Control	-2.11 ± 0.35 (-2.00)	-2.70 ± 0.01 (-2.70)	-3.59 ± 0.05 (-3.60)

The values expressed as $\bar{x}$ ± SD (median).

Radiographic crestal bone level

No peri-implant radiolucency was observed.

The differences in crestal bone loss among the study groups were statistically insignificant at the first month of observations (p > 0.05) (Table 6). Peri-implant bone loss was increasing with time. In the second month of follow-up, the highest crestal bone loss was observed around implants in the group A and comparison of the mean RCBL values with those obtained in the group B and the group C revealed a statistically significant difference (p < 0.05, respectively). The lowest crestal bone loss was recorded in the group B and comparison of these RCBL values with the values from the controls showed a statistically significant difference (p < 0.05). At this evaluation time, a higher bone loss was recorded around implants from the group C as compared with the group B, but the observed difference was statistically insignificant (p > 0.05) (Table 6). However, in the third month of observations the lowest bone loss was recorded in group C and comparison with either the group B or the group A revealed a statistically significant difference (p < 0.05). The difference in mean crestal bone loss values between the group A and controls was also statistically significant (Table 6).

Table 6

Radiographic crestal bone loss (RCBL) recorded during the first three months of loading

Experimental groups	RCBL (mm)		
	month 1	month 2	month 3
Group A	0.27 ± 0.03 (0.26)	0.32 ± 0.01 (0.32)	0.56 ± 0.01 (0.56)
Group B	0.25 ± 0.03 (0.23)	0.22 ± 0.02 (0.23)	0.36 ± 0.01 (0.36)
Group C	0.24 ± 0.02 (0.22)	0.24 ± 0.01 (0.24)	0.26 ± 0.01 (0.26)
Control	0.27 ± 0.04 (0.28)	0.30 ± 0.02 (0.30)	0.36 ± 0.01 (0.36)

The values expressed as $\bar{x}$ ± SD (median).

Removal torque

The removal torque values recorded in all the examined groups were constantly increasing during a 3-month observation period, but the statistical significance of differences between the groups followed the same pattern at each evaluation time. The highest RT values were observed in the group C and they were significantly higher than those in the group A, as well as compared with the group B, (p < 0.05, respectively). The difference in mean RT values was statistically significant between the group A and controls (p < 0.05). The lowest RT values were recorded in the group A (Table 4).

SEM analysis of broken interfaces

Observation of broken interfaces, showed the bone fragments attached to implant surfaces in all the groups. In the control group and the group A, the border of the threads had bone at different extensions (Figures 6 a and b), while, the groups B and C showed additional bone fragments inside the microgrooves.

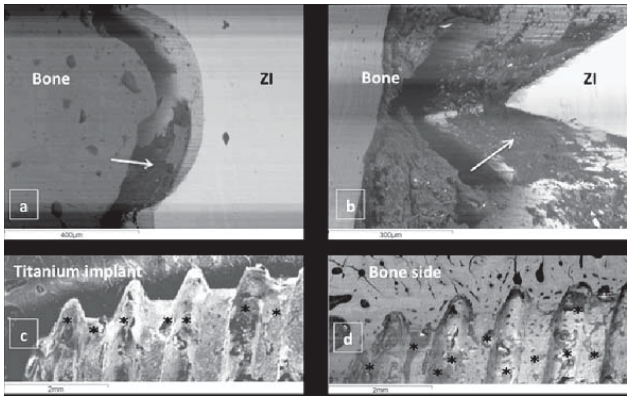

Fig. 6 – Scanning electron microscope (SEM) observation of fractured interfaces: a) backscattered image of group A, white arrow indicates fractured bone fragments adhered to bottom of interloop area of zirconia implant; b) backscattered image of the group A, top of the thread with adhered bone fragments; c) isolated control implant surfaces, black marks signaling bone fragments adhered to surface; d) isolated bone side, black marks signaling fractured bone.

Observation of the isolated bone surface showed the fractured areas of bone related to the bone fragments adhered to implant surfaces in titanium and zirconia implants (Figures 6c and 6d). Several bony growth extensions with the

same shape and dimensions of microgrooves, were observed at vertex of micro-grooved zirconia implants (Figure 7).

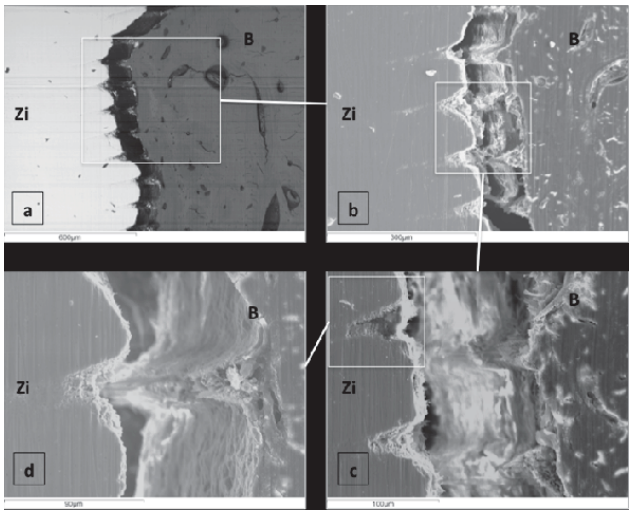

Fig. 7 – Scanning electron microscope (SEM) observation of fractured interfaces of microgrooved implants: a) backscattered image of the group C, zirconia side showing the microgrooves with bone fragments inside and bone side showing micro bone extensions with fractured tops; b) detail of microgrooves and micro bone extensions like a gear; c) and d) bone fragments inside microgroves and fractured top of bone extensions with the same shape of microgrooves, little bone residues adhered to plain zirconia surfaces could be observed.

Elemental analysis of microgrooves content revealed the presence of calcium (Figure 8).

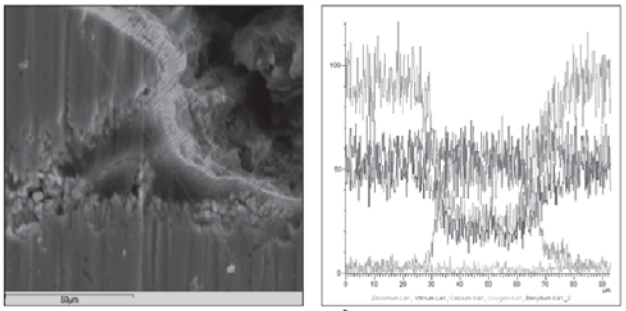

Fig. 8 – Energy dispersive X-ray spectroscopy (EDX) line scan of microgrooves showed increased calcium content inside at different levels.

Discussion

Since surface roughness could affect both mechanical and biological aspects of implant therapy, several roughness approaches have been studied [8–12, 23]. This 3-month study using a dog`s model focused on the 2 femtosecond laser-treated zirconia implants and their influence on implant stability and marginal bone level preservation. The implant collar was selected as a microstructuring target since this is the region subjected to the strongest mechanical stress once the implant is operative [24, 25]. But the intraosseous implant surface is also under stress in the apical region [26] and for this reason another study group was created in which laser processing was applied to the entire intraosseous surface. A 30 μm microstructure size was selected *a priori* in order to guide and optimize osteoblast cellular growth and to act as a cell and bone reservoir [27–29], also providing an additional increase to surface area and so possible positive effects on implant stability. The current results indicate good primary and secondary implant stability, enhanced bone tissue ingrowth as well as marginal bone preservation associated with femtosecond laser-treated zirconia implants, particularly when entire intraosseous surface has been modified.

Primary implant stability and the avoidance of micromotion are obvious necessities for undisturbed healing and successful implant treatment. It is affected not only by surgical technique and bone density at recipient site, but also degree of bone-implant contact surface determined by implant macro and micro design [30].

The implants used in the present study had the same macro geometry, with only slight differences between the (control group) titanium implant neck area (which had microthreads) and the rest. Nevertheless, insertion torque peak values registered for zirconia implants treated with laser micro-grooves over the entire surface indicate that the surface treatment produced an increase in IT due to the implants' surface roughness and micro geometry.

In the present study, the addition of microgrooves increased surface roughness by 6.5 × in the neck-processed zirconia implants and almost 12 × in the zirconia implants processed over the entire intraosseous surface and this resulted in the increase in insertion torque and decrease of PTV values. This has two possible explanations: firstly, a sufficient increase in surface roughness increases mechanical friction, and secondly, as pointed out Gedrange et al. [31], a greater bone-to-implant contact will lead to greater stability as microgrooves will produce more retentive areas and greater bone-to-implant contact.

The Periotest® was used to evaluate variations in the secondary implant stability as since resonance frequency analysis requires an abutment attachment type which zirconia implants do not have. A succession of measurements supplied information about stability behavior at different points in time. Given the animal head position, anatomical differences and the requirements of reproducible conditions the PTV values at day 0 were excluded. Thus, only after the sacrifice the extracted jaw was fixed in a holder under the same conditions and the PTV values were registered. The lower initial implant stability observed during the first month coincides with resorption and bone neoformation processes [32]. Nevertheless, the zirconia implants with the entire surface microgrooved achieved the highest stability throughout the entire study period compared with the remaining investigated implants, which may be due to the increased surface area available and increased roughness. During the second and third months implant stability rose, possibly coinciding with the calcification of the neoformed matrix. Peak occurred in the third month when mature calcified bone began to predominate.

It is believed that implant stability depends on cortical bone density and thickness [33]. In the present study, implants were placed in the molar and premolar areas of the lower jaw, in healed bone of similar intra-animal cortical thickness at all study sites. The increase in stability after 2 and 3 months may therefore be attributable, not only to stability provided by cortical bone, but also to an increase in bone-to-implant contact in the trabecular zone guided by the microgrooves.

The current study confirmed the previously described strong inverse relationship between PTV and RT, a more negative PTV, the greater value of reverse torque, and the usefulness of both to test stability.

The high removal torque values shown by all microgooved zirconia implants and titanium controls may be attributed to different factors: firstly, the controls had microthreads at the neck which increase mechanical retention, and the zirconia implants had microgrooves in all the surface, in addition an increased roughness surface, this micro geometric features could produce larger friction areas and greater bone contact along the whole length of the implant. The lack of statistical significance in the difference in PTV between the zirconia implants with microgrooves on the neck area, and the titanium controls could be related to the extension of the microgrooved area, meaning that the effects of microgrooves are reflected only with more processed surface like 10 mm processed surface of group C implants.

This is similar to the results obtained by Sennerby et al. [34] who used rabbit femurs and tibiae to evaluate RT, comparing oxidized titanium implants with surface modified coated 3.75 mm diameter zirconia implants after 6 weeks of healing. They found higher RT values with the titanium implants (59 Ncm) and the surface-modified zirconia implants (73–75 Ncm) compared to noncoated zirconia controls (18 Ncm). The authors concluded that surface modification of zirconia implants increased surface roughness and resistance to removal torque, achieving a good level of stability.

Opposed to our results, Hoffmann et al. [35] in the study on rabbits, recorded similar RT values for laser-modified zirconia implants as for the sandblasted zirconia, sintered zirconia and acid-etched titanium implants at either 6 or 12 weeks of healing. It remains unclear whether or not this result is a consequence of similar surface roughness of investigated implants because the surface topography was neither measured nor described. The lack of more distinct difference the authors explained by the fact that at the time of observation, the bone had already healed, regardless of the type of implant surface, providing similar implant stability.

Various studies carried out to date involving RT with mechanical testing of zirconia implants should be carefully compared due to the interspecies differences in the dynamics of bone healing, as well as different removal torque apparatus, implant diameters and lengths used.

SEM observation of fractured interfaces give us additional qualitative information related to bone and implant surfaces and revealed the presence of bone fragments attached to the implant surfaces demonstrating the union of titanium and zirconia with hosting bone. Higher magnification of microgrooved zirconia surfaces showed bone penetration into microgrooves. This indicates that bone can grow in small areas of 30 μm width and defined diameters. The elemental analysis within microgrooves in the sagittal section showed calcium presence in deeper zones, likely indicating the secretion of bone matrix and calcified tissue inside microgrooves.

Isolated bone surface observation showed fractured areas of bone related to the bone fragments adhered to implant surfaces in titanium and zirconia implants, in addition showed bony growth extensions with the same shape and dimensions of microgrooves, several of this fractured at vertex in microgrooved zirconia implants. All these findings, bone prolongations that form additional surface areas at microgrooved implants, the interdigitation between micro bone extensions and microgrooves, and the presence of bone fragments inside microgrooves could explain the increased stability of zirconia implants with entire microgrooved surface compared with the remaining implants.

Radiographic analysis in this study used different reference points depending on whether implants were of titanium or zirconia. Whilst titanium implants have a clearly visible platform, monobloc zirconia implants do not and so the shoulder was taken as a reference point. One difficulty of radiographic analysis of bone height around zirconia implants is the material's high radiopacity, which can make the identification of crestal bone margins difficult.

Although some clinical studies in humans have used periapical retroalveolar radiographs for evaluating crestal bone around zirconia implants [36], the measurement method used was not described. Other study on minipig maxillae has used contact microradiography to evaluate osseointegration or its lack, a technique that suffers the same difficulties as radiographic study of zirconia [37]. The image processing technique we used was chosen in order to overcome this problem, allowing us to define the uppermost part of the crestal bone as well as the implant edges, with increased image clarity, eliminating the chance of superimposed images.

The results of this 3-month study revealed improved maintenance of crestal bone level around microgrooved implants in comparison with microthreaded implants (titanium controls) and particularly with rough neck implants without microthreading (sand blasted zirconia). Although microthreads at implant neck transform the shear force between the implants and crestal bone into the compressive force to which bone is the most resistant allowing preservation of bone tissue, addition of microgrooves that interlock the adjacent bone seems to be more efficient [38]. However, there are several limitations of the present study. Differences in implant-abutment junction between the investigated implants (all zirconia implants were one-piece whereas titanium controls were two-piece implants but placed in one-stage manner) could possibly affect crestal bone level. Therefore, the greater bone loss noted around the titanium implants could be due to the presence of a microgap that allows accumulation of debris and bacteria that cause inflammation and could not be attributed only to the lack of microgrooves [39]. The

other limitation is the short-term follow up period (3 months after functional loading) that is insufficient for marginal bone stabilization because the most critical period of the bone level changes occurs 1 year after loading [40].

Conclusion

Within the limitations of the present study on dogs´ mandibles it may be concluded that addition of microgrooves on the surface of zirconia dental implants by means of laser ablation enhances primary and secondary implant stability, promotes bone tissue ingrowth and preserves crestal bone level after a 3-month follow-up. This could be attributed to the increased implant surface roughness and reduced presence of contaminants following laser microtexturing. Mechanical and biological advantages of this surface modification are even more pronounced when applied to the entire intraosseous surface of zirconia implants.

R E F E R E N C E S

1. *Andreiotelli M, Wenz HJ, Kohal R.* Are ceramic implants a viable alternative to titanium implants? A systematic literature review. Clin Oral Implants Res 2009; 20(Suppl 4): 32−47.
2. *Piconi C, Maccauro G.* Zirconia as a ceramic biomaterial. Biomaterials 1999; 20(1): 1−25.
3. *Albrektsson T, Sennerby L, Wennerberg A.* State of the art of oral implants. Periodontol 2008; 47: 15−26.
4. *Scarano A, Di CF, Quaranta M, Piattelli A.* Bone response to zirconia ceramic implants: an experimental study in rabbits. J Oral Implantol 2003; 29(1): 8−12.
5. *Kohal RJ, Wolkewitz M, Hinze M, Han J, Bächle M, Butz F.* Biomechanical and histological behavior of zirconia implants: an experiment in the rat. Clin Oral Implants Res 2009; 20(4): 333−9.
6. *Davies JE.* Mechanisms of endosseous integration. Int J Prosthodont 1998; 11(5): 391−401.
7. *Aloy-Prósper A, Maestre-Ferrín L, Peñarrocha-Oltra D, Peñarrocha-Diago M.* Marginal bone loss in relation to the implant neck surface: an update. Med Oral Patol Oral Cir Bucal 2011; 16(3): e365−8.
8. *Langhoff JD, Voelter K, Scharnweber D, Schnabelrauch M, Schlottig F, Hefti T,* et al. Comparison of chemically and pharmaceutically modified titanium and zirconia implant surfaces in dentistry: a study in sheep. Int J Oral Maxillofac Surg 2008; 37(12): 1125−32.
9. *Gahlert M, Röhling S, Wieland M, Sprecher CM, Kniha H, Milz S.* Osseointegration of zirconia and titanium dental implants: a histological and histomorphometrical study in the maxilla of pigs. Clin Oral Implants Res 2009; 20(11): 1247−53.
10. *Lee J, Sieweke JH, Rodriguez NA, Schüpbach P, Lindström H, Susin C,* et al. Evaluation of nano-technology-modified zirconia oral implants: a study in rabbits. J Clin Periodontol 2009; 36(7): 610−7.
11. *Ferguson SJ, Langhoff JD, Voelter K, Rechenberg B, Scharnweber D, Bierbaum S,* et al. Biomechanical comparison of different surface modifications for dental implants. Int J Oral Maxillofac Implants 2008; 23(6): 1037−46.
12. *Pirker W, Kocher A.* Immediate, non-submerged, root-analogue zirconia implants placed into single-rooted extraction sockets: 2-year follow-up of a clinical study. Int J Oral Maxillofac Surg 2009; 38(11): 1127−32.
13. *Delgado-Ruíz RA, Calvo-Guirado JL, Moreno P, Guardia J, Gomez-Moreno G, Mate-Sánchez JE,* et al. Femtosecond laser microstructuring of zirconia dental implants. J Biomed Mater Res B Appl Biomater 2011; 96(1): 91−100.
14. *Lu J, Rao MP, MacDonald NC, Khang D, Webster TJ.* Improved endothelial cell adhesion and proliferation on patterned titanium surfaces with rationally designed, micrometer to nanometer features. Acta Biomater 2008; 4(1): 192−201.
15. *Lamers E, Horssen R, Riet J, Delft CF, Luttge R, Walboomers XF,* et al. The influence of nanoscale topographical cues on initial osteoblast morphology and migration. Eur Cell Mater 2010; 20: 329−43.
16. *Loesberg WA, Riet J, Delft FC, Schön P, Figdor CG, Speller S,* et al. The threshold at which substrate nanogroove dimensions may influence fibroblast alignment and adhesion. Biomaterials 2007; 28(27): 3944−51.
17. *Lamers E, Walboomers FX, Domanski M, Riet J, Delft FC, Luttge R,* et al. The influence of nanoscale grooved substrates on osteoblast behavior and extracellular matrix deposition. Biomaterials 2010; 31(12): 3307−16.
18. *Klein MO, Bijelic A, Toyoshima T, Götz H, Koppenfels RL, Al-Nawas B,* et al. Long-term response of osteogenic cells on micron and submicron-scale-structured hydrophilic titanium surfaces: sequence of cell proliferation and cell differentiation. Clin Oral Implants Res 2010; 21(6): 642−9.
19. *Abrahamsson I, Berglundh T.* Tissue characteristics at microthreaded implants: an experimental study in dogs. Clin Implant Dent Relat Res 2006; 8(3): 107−13.
20. *Nevins M, Nevins ML, Camelo M, Boyesen JL, Kim DM.* Human histologic evidence of a connective tissue attachment to a dental implant. Int J Periodontics Restorative Dent 2008; 28(2): 111−21.
21. *Weiner S, Simon J, Ehrenberg DS, Zweig B, Ricci JL.* The effects of laser microtextured collars upon crestal bone levels of dental implants. Implant Dent 2008; 17(2): 217−28.
22. *Pecora GE, Ceccarelli R, Bonelli M, Alexander H, Ricci JL.* Clinical evaluation of laser microtexturing for soft tissue and bone attachment to dental implants. Implant Dent 2009; 18(1): 57−66.
23. *Rocchietta I, Fontana F, Addis A, Schupbach P, Simion M.* Surface-modified zirconia implants: tissue response in rabbits. Clin Oral Implants Res 2009; 20(8): 844−50.
24. *Shin S, Han D.* Influence of a microgrooved collar design on soft and hard tissue healing of immediate implantation in fresh extraction sites in dogs. Clin Oral Implants Res 2010; 21(8): 804−14.
25. *Geng JP, Ma QS, Xu W, Tan KB, Liu GR.* Finite element analysis of four thread-form configurations in a stepped screw implant. J Oral Rehabil 2004; 31(3): 233−9.
26. *Faegh S, Müftü S.* Load transfer along the bone-dental implant interface. J Biomech 2010; 43(9): 1761−70.
27. *Marotti G, Zallone AZ, Ledda M.* Number, size and arrangement of osteoblasts in osteons at different stages of formation. Calcif Tissue Res 1976; 21(Suppl): 96−101.
28. *Zallone AZ.* Relationships between shape and size of the osteoblasts and the accretion rate of trabecular bone surfaces. Anat Embryol (Berl) 1977; 152(1): 65−72.
29. *Puckett S, Pareta R, Webster TJ.* Nano rough micron patterned titanium for directing osteoblast morphology and adhesion. Int J Nanomedicine 2008; 3(2): 229−41.
30. *Martinez H, Davarpanah M, Missika P, Celletti R, Lazzara R.* Optimal implant stabilization in low density bone. Clin Oral Implants Res 2001; 12(5): 423−32.
31. *Gedrange T, Hietschold V, Mai R, Wolf P, Nicklisch M, Harzer W.* An evaluation of resonance frequency analysis for the determination of the primary stability of orthodontic palatal im-

plants. A study in human cadavers. Clin Oral Implants Res 2005; 16(4): 425−31.

32. *Chang P, Lang NP, Giannobile WV*. Evaluation of functional dynamics during osseointegration and regeneration associated with oral implants. Clin Oral Implants Res 2010; 21(1): 1−12.
33. Rozé J, Babu S, Saffarzadeh A, Gayet-Delacroix M, Hoornaert A, Layrolle P. Correlating implant stability to bone structure. Clin Oral Implants Res 2009;20(10):1140-1140.
34. *Sennerby L, Dasmah A, Larsson B, Iverhed M*. Bone tissue responses to surface-modified zirconia implants: A histomorphometric and removal torque study in the rabbit. Clin Implant Dent Relat Res 2005;7(Suppl 1): S13−20.
35. *Hoffmann O, Angelov N, Zafiropoulos G, Andreana S*. Osseointegration of zirconia implants with different surface characteristics: an evaluation in rabbits. Int J Oral Maxillofac Implants 2012; 27(2): 352−8.
36. *Oliva J, Oliva X, Oliva JD*. One-year follow-up of first consecutive 100 zirconia dental implants in humans: a comparison of 2 different rough surfaces. Int J Oral Maxillofac Implants 2007; 22(3): 430−5.
37. *Gahlert M, Gudehus T, Eichhorn S, Steinhauser E, Kniha H, Erhardt W*. Biomechanical and histomorphometric comparison between zirconia implants with varying surface textures and a titanium implant in the maxilla of miniature pigs. Clin Oral Implants Res 2007; 18(5): 662−8.
38. *Jung YC, Han CH, Lee KW*. A 1-year radiographic evaluation of marginal bone around dental implants. Int J Oral Maxillofac Implants 1996; 11(6): 811−8.
39. *Hermann JS, Schoolfield JD, Schenk RK, Buser D, Cochran DL*. Influence of the size of the microgap on crestal bone changes around titanium implants. A histometric evaluation of unloaded non-submerged implants in the canine mandible. J Periodontol 2001; 72(10): 1372−83.
40. *Lee D, Choi Y, Park K, Kim C, Moon I*. Effect of microthread on the maintenance of marginal bone level: a 3-year prospective study. Clin Oral Implants Res 2007; 18(4): 465−70.

Received on October 3, 2012.
Revised on November 21, 2012.
Accepted on November 27, 2012.
OnLine-First July, 2013 .